Atmospheric Pollution Research 14 (2023) 101670

Contents lists available at ScienceDirect

Atmospheric Pollution Research

journal homepage: www.elsevier.com/locate/apr

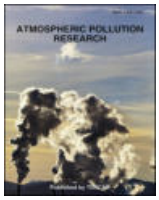

Spatial-temporal assessment of air quality in Rome (Italy) based on anemological clustering

Annalisa Di Bernardino [a,*], Anna Maria Iannarelli [b], Stefano Casadio [b], Giovanna Pisacane [c], Anna Maria Siani [a]

[a] Sapienza University of Rome, Department of Physics, Rome, Italy
[b] SERCO SpA, Frascati, Italy
[c] Climate Modeling and Impacts Laboratory, ENEA-Casaccia Research Center, Rome, Italy

ARTICLE INFO

Keywords:
Cluster analysis
Air pollution
In-situ measurements
Ozone
Nitrogen oxides
Particulate matters

ABSTRACT

The relationship between atmospheric circulation and air pollution is investigated by analysing in-situ measurements collected at four monitoring stations located in the coastal area of central Italy over the period 2014–2020. The study is based on the prior identification of three typical circulation patterns, obtained via the k-mean clustering of surface anemological data. The present analysis explores the relation between atmospheric dynamics and concentrations of nitrogen oxides (NO and NO_2), NO_2/NO_x ($NO_x = NO + NO_2$), ozone (O_3), and particulate matters ($PM_{2.5}$ and PM_{10}). When local circulation systems prevail, the best air quality conditions are observed, as the onset of the sea breeze permits clean, marine air masses to be advected to the urban area of Rome. On the other hand, when synoptic winds persistently blow from the northeast, the highest concentrations of atmospheric pollutants are recorded. Finally, when both synoptic and local winds blow from the southeast, the complex anemological regime results in low ventilation and quite poor air quality conditions. The largest differences among clusters are observed during winter, when the north-easterly winds can persist for more than ten consecutive days, with the enhanced atmospheric stability limiting the development of the mixed layer, causing the increase of ground-level pollutants concentration.

1. Introduction

Air pollution has been recognised to be a major environmental risk, with significant impacts on human health, especially in urbanised areas (European Environmental Agency, 2021). The report shows that, in 2019, more than 300,000 premature deaths in Europe are attributable to direct or indirect exposure to $PM_{2.5}$ (atmospheric particles with an aerodynamic diameter less than 2.5 μm), over 40,000 deaths can be related to high values of nitrogen dioxide (NO_2), and nearly 17,000 to extreme ozone (O_3) concentrations. The reported mortality impacts represent an intolerable social cost, alongside with negative economic consequences of augmented healthcare expenditures and lower productivity due to reduced workforce well-being, which can only be offset in a longevity-economy approach (Mujtaba and Shahzad, 2021; Scott, 2021). In addition to health issues (e.g., respiratory diseases, cardiovascular problems, and stroke), excessive levels of key atmospheric pollutants, such as Sulphur dioxide (SO_2) and O_3, are responsible for negative impacts on sensitive ecosystems, e.g., exacerbating the processes of acidification/eutrophication and limiting biodiversity (Lovett et al., 2009). Due to the severe impact of air pollution on human health and the environment, international governmental agencies have ratified regulations to limit pollutant emissions and develop environmental risk mitigation and adaptation strategies. Specifically, the European Directive 1999/30/EC (EU, 1999) and, more recently, the European Air Quality Directive 2008/50/EC (EU, 2008) set the legal limits for the main atmospheric pollutants, i.e., O_3, NO_2, $PM_{2.5}$, SO_2, benzene (C_6H_6), carbon monoxide (CO), and particulate matter with aerodynamic diameter below 10 μm (PM_{10}), while, to date, no limits are prescribed for the atmospheric concentrations of nitrogen monoxide (NO), and nitrogen oxides ($NO_x = NO + NO_2$). In recent years, national and international institutions have also actively pursued the reduction of air pollution and energy consumption (e.g., through incentives for the purchase of low-emission vehicles, energy requalification of buildings, and innovative energy policies, among others). Nonetheless, no

Peer review under responsibility of Turkish National Committee for Air Pollution Research and Control.
* Corresponding author.
E-mail address: annalisa.dibernardino@uniroma1.it (A. Di Bernardino).

https://doi.org/10.1016/j.apr.2023.101670
Received 4 November 2022; Received in revised form 11 January 2023; Accepted 31 January 2023
Available online 1 February 2023

substantial improvements in the air quality levels in many European areas have yet been observed (European Environmental Agency, 2021).

An in-depth analysis of all the factors governing atmospheric pollution is necessary to reliably weigh the trade-offs of alternative policies, and adopt optimal mitigation actions, by discriminating among the contributions from anthropogenic and natural sources (Lelieveld et al., 2015), chemical processes, orography, and meteorological conditions. Specifically, in the atmospheric boundary layer, the wind is one of the forcings that most affects the air quality, as it controls the dispersion and diffusion of pollutants near the ground (Xie et al., 2022). In fact, weak winds and persistent atmospheric stability can favour the accumulation of pollutants (Kukkonen et al., 2005) while, on the contrary, strong winds can improve or worsen the air quality depending on whether they bring clean air masses or transfer pollutants from upwind regions (Yu et al., 2020). Therefore, determining the regional meteorological and anemological types can support the identification of emergency measures during episodes of heavy pollution (Jia et al., 2017). The classification of weather types has been widely used in the last century, yet only recent technological developments have allowed switching from subjective to objective classification methods, that is from arrangements based on the visual analysis of weather systems on synoptic maps (Lamb, 1972; Hess and Brezowsky, 1977), to semi-automatic or automatic clustering techniques that allow grouping data based on their common measurable characteristics (Jain et al., 1999). As pointed out in the review by Govender and Sivakumar (2020), the clustering approach has been widely applied to atmospheric physics and air pollution. For instance, Kijewska and Bluszcz (2016) applied clustering techniques to investigate the differences among European countries in terms of *per capita* greenhouse gases emissions; Hsu and Cheng (2019) identified six characteristic synoptic circulation patterns by studying the daily-averaged wind intensity, wind direction, and sea-level pressure in Taiwan, also discussing implications on pollution. Moreover, Tian et al. (2020) applied clustering to $PM_{2.5}$, SO_2, NO_2, CO, and O_3 concentrations in order to study their spatial and temporal distribution in Northern China. In Italy, recent applications of cluster analysis to the output of high-resolution regional climate models led to the identification of typical climate zones (Calmanti et al., 2015). Furthermore, Riccio et al. (2007) and Squizzato and Masiol (2015) used a clustering approach based on the analysis of backward trajectories to evaluate the effects of atmospheric dynamics on air quality in different Italian cities.

In this study, we propose the application of cluster analysis to investigate the impact of synoptic and local scale anemological conditions on atmospheric pollutant concentrations. To this purpose, we consider the pollutant concentrations measured at four in-situ air quality stations located in the centre of Rome (Italy), a densely populated and highly polluted area, and in its rural surroundings over the period 2014–2020. Furthermore, the relationship between pollutant concentrations and the persistence of specific anemological conditions, that is, of a specific cluster, is explored.

The paper is structured as follows: Sect. 2 presents the data and methods adopted, focusing on the description of the area of interest, the pollutant concentration dataset, and the description of the prevailing synoptic and local circulation patterns, as identified through the clustering procedure in Di Bernardino et al. (2022a). The results of the study are presented and discussed in Sects. 3 and 4, respectively. Finally, the main findings are summarised in Sect. 5.

2. Data and methods

2.1. General description of the area under investigation

The area of interest for the proposed analysis is a portion of the Lazio

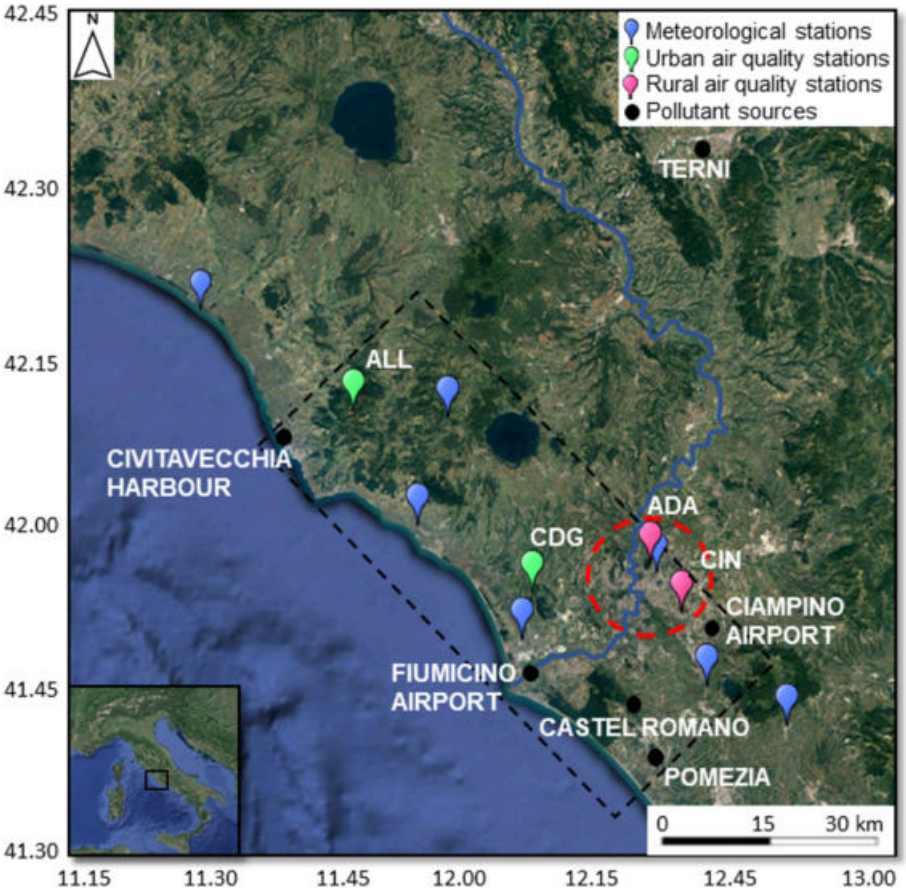

Fig. 1. Geographical map of the region of interest for this study. The dashed black line depicts the investigated domain, the red dashed circle highlights the urban area of Rome, the blue line shows the Tiber River, flowing along the Tiber Valley, and the black dots identify the main atmospheric pollutants sources of the region. The urban (magenta markers) and rural (green markers) air quality stations are depicted, together with the weather stations (blue markers) used for the anemological clustering.

region (see dashed black line in Fig. 1, Lat. 11.70°–12.50°, Lon. 41.60°–42.30°, surface of about 2200 km^2), located along the coast of the Tyrrhenian Sea in central Italy. The selected area is analogous to that already considered in Di Bernardino et al. (2022a). Topographically, the area is mainly flat near the coast and along the Tiber Valley (cyan line in Fig. 1), which stretches northeast of the capital, and is surrounded by hills to the north (Monti della Tolfa, Monti Sabatini, and Monti Cimini) and to the south (Monti Lepini and Colli Albani). Following the Köppen-Geiger climate classification, this region belongs to the hot-summer Mediterranean climate class (Csa), experiencing a temperate climate, with dry and hot summers (Beck et al., 2018).

The city of Rome (Lat. 41.90°, Lon. 12.50°, see red circle in Fig. 1), the capital of Italy and the third most populous metropolis in Europe, hosts approximately 4.3 million citizens in the metropolitan area (ISTAT, 2020). In the city centre, the main economic activities concern services and commerce, with no significant industrial activities. Nevertheless, the city is frequently subject to severe pollution events, with important impacts on both environment and human health (Palmieri et al., 2008; Di Bernardino et al., 2021a). The main atmospheric pollutant sources are the emissions from vehicular traffic and domestic heating. The major industrial districts, as shown in Fig. 1, are Pomezia (Lat. 41.67°, Lon. 12.50°) and Castel Romano (Lat. 41.71° Lon. 12.44°), located south of Rome. Furthermore, important pollution sources are the international airports of Fiumicino (Lat. 41.79°, Lon. 12.25°) and Ciampino (Lat. 41.80°, Lon. 12.59°), located about 30 km southwest and 14 km southeast of Rome, respectively. Maritime traffic is mainly conveyed to the Civitavecchia harbour (Lat. 42.10°, Lon. 11.78°), northwest of Rome. Moreover, in the case of northerly winds, the air quality in Rome can worsen because of industrial emissions produced by the neighbouring city of Terni (Lat. 42.55°, Lon. 12.64°, about 75 km northeast of Rome), where one of the largest steel plants nationwide is located. Industrial emissions can be conveyed to Rome along the Tiber Valley.

2.2. Surface air pollutants dataset

To evaluate the impact of atmospheric dynamics on air pollution dispersion/accumulation, four stations belonging to the air quality monitoring network managed by the Regional Agency for Environmental Protection (ARPA Lazio) were considered (Fig. 1). The air quality stations were selected on the basis of their location, in downtown Rome and in the rural surrounding areas, and on the data availability for the analysed period. Moreover, they are located in the same area already covered by the anemological clustering presented in Di Bernardino et al. (2022a), i.e., they are positioned within 30 km from the coastline, and are in operation since 2014 (details in Table 1). The Villa Ada (hereinafter, ADA) and Cinecittà (CIN) stations are classified by ARPA Lazio as urban background stations and have been identified as representative of the pollution conditions in the urban environment. The Castel di Guido (CDG) and Allumiere (ALL) stations have been selected to characterise the rural background conditions, by being located far from inhabited centres and therefore not directly influenced by local emissions. However, such a broad classification does not account for the peculiarities of each station: CIN and ADA are indeed both situated within the urban perimeter, yet ADA is located on the edge of Rome's largest green area (Villa Ada), where the direct impact of local emissions is negligible, while CIN, despite its lying along a road characterised by low traffic levels, can be affected by the emissions advected from the Ciampino airport by southerly winds. On the other hand, as both stations are located along the Tiber Valley, they can be simultaneously affected by the channelling of persistent northerly winds, transporting pollutants from the north-eastern quadrant of the capital. The CDG station, which is situated in a protected natural area, is also subject to the advection of chemicals from distant sources, in particular from the Fiumicino airport, located 10 km to the south. In its turn, the rural ALL station, which lies on the edge of a large beech forest, about 11 km northeast of the Civitavecchia harbour, can detect pollutants emitted by ships and advected by the sea breeze.

The observational sites provide measurements of the daily-averaged concentrations of NO, NO_2, O_3, PM_{10}, and $PM_{2.5}$, the latter only missing for the ALL station. ARPA Lazio guarantees that all data are quality checked, although information about the associated errors is not currently available. Sensors are calibrated following the guidelines issued by the Italian Institute for Environmental Protection and Research (Istituto Superiore per la Protezione e la Ricerca Ambientale – ISPRA) (ISPRA, 2014), as required by the Legislative Decree March 30, 2017 GU n. 96 (Ministry for Environment, Land and Sea Protection of Italy, 2017).

In addition to the measurements of individual species provided by the monitoring network, the NO_2 to NO_x ratio was computed. The latter is an important indicator of the state of the photo-catalytic equilibrium (Ravina et al., 2022) and is typically assumed as a surrogate in dispersion models in estimating NO_x emissions in urban environments (Xiang et al., 2022). In near road-environments, NO_2/NO_x typically assumes values between 0 and 0.1 for low emissions vehicles and between 0.7 and 1 in vehicles with diesel particulate filters or trucks with unknown emissions control technology (Richmond-Bryant et al., 2017).

2.3. Anemological pattern clustering

The classification of the circulation regimes that characterise the region under investigation is based on the clustering procedure described in Di Bernardino et al. (2022a), which allows discriminating between the alternative synoptic and local circulation patterns affecting air quality in the urban area of Rome and its rural surroundings. In Di Bernardino et al. (2022a), the classification was carried out by applying the k-means clustering algorithm, proposed by Hartigan and Wong (1979), to the hourly-averaged wind speed and direction measured at seven surface meteorological stations located within a maximum distance of 30 km from the coast (including downtown Rome).

Since the focus of the paper was the identification of the circulation patterns in a coastal environment and of the link between the synoptic and the local scale circulation, the authors introduced additional vari-

Table 1
Summary of the features of ARPA Lazio stations (location, environmental classification, and variables collected).

Station ID	Station name	Lat. (°)	Lon. (°)	Elevation (m a.s.l.)	Station classification	Variables
ADA	Villa Ada	41.93	12.51	50	urban background	NO, NO_2 O_3 $PM_{2.5}$, PM_{10}
CIN	Cinecittà	41.86	12.57	53	urban background	NO, NO_2 O_3 $PM_{2.5}$, PM_{10}
ALL	Allumiere	42.16	11.91	542	rural background	NO, NO_2 O_3 PM_{10}
CDG	Castel di Guido	41.89	12.27	61	rural background	NO, NO_2 O_3 $PM_{2.5}$, PM_{10}

ables, leading to an optimal set of seven parameters.

(i) u_{morn}, average zonal wind component in the period 08:00–12:00 UTC;
(ii) v_{morn}, average meridional wind component in the period 08:00–12:00 UTC;
(iii) u_{after}, average zonal wind component in the period 15:00–18:00 UTC;
(iv) v_{after}, average meridional wind component in the period 15:00–18:00 UTC;
(v) R;
(vi) $\cos(\theta)$;
(vii) $\sin(\theta)$.

The time intervals 08:00–12:00 UTC and 15:00–18:00 UTC represent the average periods during which the sea breeze regime develops and ceases in the selected region, respectively, while R is the recirculation factor, given by the ratio between the transport distance and the wind run (Allwine and Whiteman, 1994), and θ is the wind rotation angle, measured clockwise starting from the North.

By applying both the "elbow" and the "silhouette" methods (Kodinariya and Makwana, 2013), three clusters were identified, exhibiting the following key features.

(i) the Northeasterly cluster (NEC) is dominated by synoptic conditions and characterised by prevailing winds from the Northeast throughout the day. In this case, a high-pressure system located over the North Sea and a low-pressure system over the Balkans lead to wind convergence over Italy. As evidenced by the weak wind intensity, days of atmospheric stagnation likely belong to this pattern;
(ii) the Sea Breeze Cluster (SBC) is observable when the local scale circulation dominates over central Italy. During the central hours of the day an increase in wind speed, blowing perpendicularly to the coastline, is discernible;
(iii) the Southeasterly Cluster (SEC) is detectable when the Italian Peninsula is crossed by a high-pressure gradient and the wind blows from the southeast quadrant throughout the day. In this case, the synoptic and local circulations overlap, and the development of the sea breeze determines an increase in wind intensity and a slight rotation of the wind direction in the central hours of the day. This condition favours Saharan dust outbreaks.

In Fig. 2, the hourly trends of wind speed and direction for the three clusters identified in Di Bernardino et al. (2022a) are shown. The plots illustrate the average anemological conditions referred to each cluster centroid, over the entire population of each cluster.

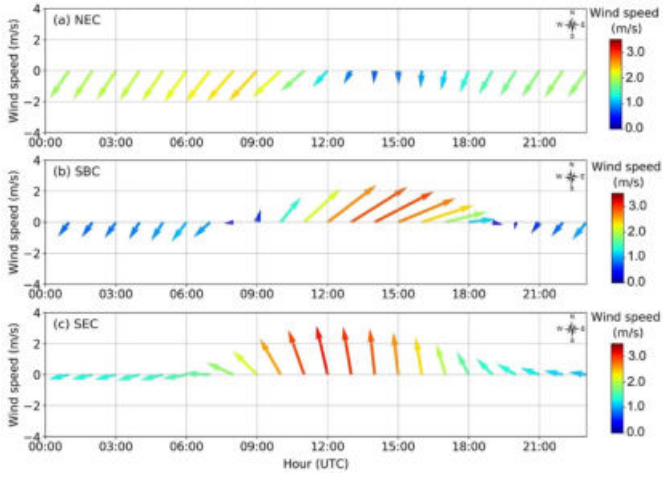

Fig. 2. Daily trend of average wind speed (colours and vectors length, m/s) and wind blowing direction (vectors orientation) for the three clusters (adapted from Di Bernardino et al., 2022a).

2.4. Significance assessment of the clustering procedure

After the preliminary analysis of pollutant time-series characteristics presented in Section 3.1, the link between local pollution levels and prevailing anemological conditions identified is assessed by distributing measurement among the three clusters NEC, SBC, and SEC, according to the concurrent wind observations at each station, for the whole investigation period. Days that could not be associated with a specific cluster due to missing wind data were discarded from the analysis.

The statistical significance of such distribution is assessed by applying the Mann Whitney *U* test to the resulting set of time series. The Mann Whitney *U* test is a non-parametric procedure typically used to verify that two independent samples do not in fact belong to the same statistical population, by assessing the probability that a randomly drawn observation from one group is larger than a randomly drawn observation from the other (Mann and Whitney, 1947; Wilcoxon, 1949). In this case, the two independent samples are alternatively represented by one of the three distinct pairs (NEC, SBC), (NEC, SEC), and (SBC, SEC), and a 95% significance level is required to back test that clusters are actually representative of distinct anemological conditions.

Moreover, in order to verify any possible correlation between the concentrations of each individual pollutant measured in the stations analysed, the correlation matrices, reporting the standard Pearson correlation coefficient and the associated p-values are computed (not shown). The correlation coefficient is very low (less than 0.09) for each pollutant and for each pair of stations and the p-value is below the statistical significance level of $p = 0.05$ only in a few cases (NO_2: CIN-CDG; O_3: ADA-ALL), suggesting a poor correlation between the concentrations measured at the selected sites.

3. Results

3.1. Multi-year characterisation of air pollutant concentrations

Fig. 3 shows the monthly-averaged time series of the atmospheric pollutant concentrations measured at the selected stations. For each site, the corresponding averages over the period 2014–2020 are presented in Table 2, together with the associated detrended and deseasonalised standard deviations (STDs), as a measure of the variability induced by short-term processes. STD deseasonalising (via phase averaging) avoids the anthropogenic signal being obscured by the natural variability of concentrations, which can be inflated by the marked seasonal cycle of atmospheric species, especially those (e.g., O_3) that are subject to photochemical reactions (Fountoulakis et al., 2019). Similarly, detrending allows filtering out the effects of long-term variations that are not directly induced by the persistence of meteorological patterns (Di Bernardino et al., 2022b). Long-term trends were assessed via a linear regression analysis of the daily time series of pollutants concentrations and subtracted from the original series. Finally, Table S1 reports the absolute maxima daily-averaged concentrations of species over the period of interest, together with their date of observation.

NO (Fig. 3a) exhibits a coherent seasonal cycle at all stations, with more marked oscillations in the urban sites with respect to the rural ones. In particular, CIN reached a maximum concentration of 251.0 μg/m^3 in December 2015 (Table S1), about +145% compared to ADA. This result suggests, as pointed out in Sect 2.2, that the classification of monitoring stations provided by ARPA Lazio does not account for the environmental characteristics of each station. In rural stations, both monthly concentrations and daily absolute maxima are significantly lower than in downtown Rome, with an almost imperceptible seasonal variation.

The temporal behaviour of NO_2 (Fig. 3b) is comparable to that of NO,

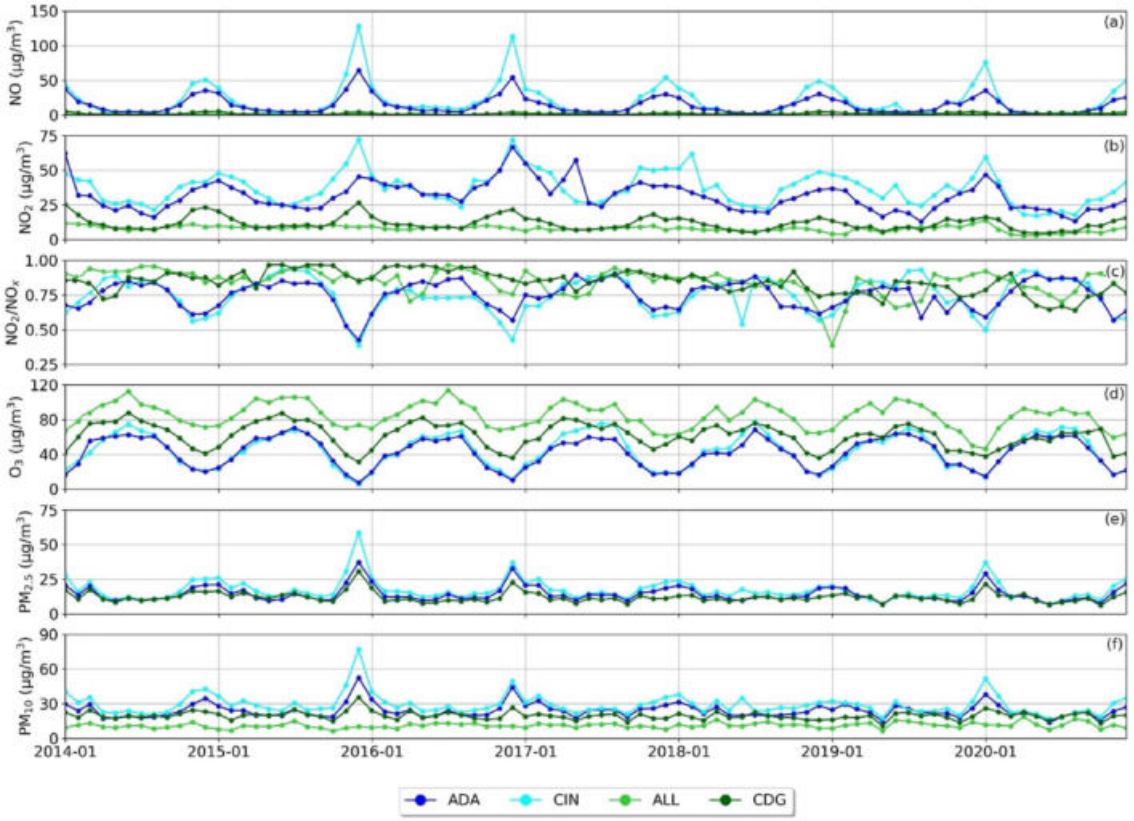

Fig. 3. Time series of monthly-averaged pollutant concentrations for the selected stations over the period 2014–2020.

Table 2
Average concentrations and deseasonalised STDs (in square brackets) for the selected station over the period 2014–2020.

Stat. ID	NO (µg/m^3)	NO_2 (µg/m^3)	NO_2/NO_x	O_3 (µg/m^3)	$PM_{2.5}$ (µg/m^3)	PM_{10} (µg/m^3)
ADA	14.4 [8.5]	31.6 [8.9]	0.8 [0.2]	42.5 [9.5]	14.2 [5.6]	24.1 [7.6]
CIN	20.9 [15.4]	37.4 [9.9]	0.8 [0.2]	44.4 [9.9]	17.0 [7.1]	29.2 [10.5]
ALL	1.5 [1.0]	8.1 [2.4]	0.9 [0.1]	84.7 [8.4]	–	11.3 [4.8]
CDG	2.1 [1.6]	11.9 [4.7]	0.9 [0.1]	62.1 [10.3]	12.0 [5.2]	19.9 [6.6]

although the average concentrations are always below 75.0 µg/m^3 and maximum daily concentrations do not exceed 106.0 µg/m^3. As for NO, the highest NO_2 concentrations are recorded in the urban background stations, reaching higher values at CIN than at ADA. The urban sites show marked seasonal fluctuations, which tend to disappear in the rural environment. In particular, ALL always exhibits minimum concentrations below 14 µg/m^3.

NO_2/NO_x (Fig. 3c) is affected by significant temporal and spatial variability. On average, urban stations experience a marked seasonal cycle with ratios between 0.40 and 0.99. In rural areas, NO_2/NO_x shows limited variations, reaching higher values than in Rome's city centre. Regardless of the urbanization level, all the stations measured the highest (lowest) ratios in summer (winter). The results are in agreement with values found in previous studies: e.g., Bower et al. (1993) observed that NO_2/NO_x ranges between 0.17 and 0.5 at the kerbside, 0.47 and 0.59 at urban background sites, and reaches about 0.85 at rural stations. The higher values assumed in rural sites are due to the dilution of NO_x as the distance from the emission sources increases and to the greater availability of O_3. On the contrary, the lower ratios observed in urban environments are related to the proximity of primary NO_2 sources, mainly due to diesel-fuelled vehicles (Carslaw et al., 2011). In addition, as highlighted by Williams and Carslaw (2011), exhaust gas treatment devices used for reducing particulate matter missions by diesel vehicles can be responsible for the increasing fraction of primary NO_2 in NO_x.

The O_3 time series (Fig. 3d) shows a reversed seasonal cycle with respect to that of NO and NO_2: in Rome, both relative and absolute maxima are recorded in summer, as a consequence of the temperature-enhanced photochemical chain reaction. At ALL concentrations are on average 30% higher than at the other stations, with less pronounced seasonal variability.

The time evolution of $PM_{2.5}$ concentrations (Fig. 3e) is very similar across the stations, regardless of their location and a generally limited seasonal cycle. In correspondence of the autumn/winter relative maxima (possibly associated with the stagnation of particulate matter in the layer of the atmosphere closest to the ground as a consequence of the limited development of the mixed layer), differences between stations become more marked.

On the other hand, the otherwise similar evolution of PM_{10} concentrations (Fig. 3f) exhibits higher variability and clearer differences between stations in correspondence of both the main (cold season) and secondary (warm season) maxima. The lowest PM_{10} monthly concentrations are sustainedly recorded at ALL, a score that can be also expected to locally characterise $PM_{2.5}$ measurements, although such conjecture cannot be verified due to missing data. Nevertheless, the hypothesis of lowest particulate concentrations being a specific feature of rural sites might be inferred from the observations at CDG, the other rural station, where both PM_{10} and $PM_{2.5}$ are measured and concentrations are found to be consistently lower than at all other locations, even during the cold season.

The seasonal variability of atmospheric pollutant concentrations suggests a threefold explanation.

(i) As expected, all pollutants directly influenced by anthropic emissions, such as NO, NO_2, PM_{10}, and, to a lesser extent, $PM_{2.5}$ exhibit higher average concentrations in downtown Rome due to the proximity of emission sources. Moreover, measurements are collected close to the ground and, therefore, are strictly connected to local sources: during winter, pollution from domestic heating is added to the emissions of vehicular traffic worsening the air quality, while during the summer holidays, when many commercial and industrial activities are closed or have reduced production (ISTAT, 2021), lower pollutant concentrations are measured, except for O_3, which mainly responds to temperature. The NO_2 and NO peaks recorded during the warm season could be related to local and short-term phenomena, such as fires, for which detailed information can only be acquired from local news reports.

(ii) Exceptional concentrations of particulate matter can be related to impulsive phenomena. For instance, occasional high daily concentrations of $PM_{2.5}$ and PM_{10} in December and January have been attributed to the combination of persistent atmospheric stability and increased particulate emissions from fireworks, the latter being ascribable to New Year celebrations (Reuters, 2015). This might indeed be the case for the $PM_{2.5}$ peak measured at all stations on January 3, 2016 (ARPA Lazio, 2016). Peaks in PM_{10} and $PM_{2.5}$ are also recorded when outbursts of air masses from North Africa reach the region, transporting large amounts of suspended dust, as is the case of the PM_{10} maximum observed on December 1, 2014 (ARPA Lazio, 2014). When suspended particles penetrate the boundary layer, they can deposit on the ground, and consequently deteriorate the air quality of the adjacent atmospheric layer (Gobbi et al., 2013).

(iii) In the geographic area considered, cold months (typically from November to March) are characterised by recurrent events of persistent atmospheric stability, giving rise to atmospheric stagnation, and limiting the diurnal development of the mixed layer. This implies a limited dispersion of contaminants, which remain trapped in the atmospheric layer closest to the ground, exacerbating air pollution in the city. E.g., during December 2015, persistent high-pressure conditions caused fog and low temperatures over the Italian peninsula, resulting in very high NO, NO_2 and PM concentrations. Furthermore, during the winter months, the frequent northerly winds can convey pollutants emitted north of Rome into the Tiber Valley, adding up to local emissions and worsening the air quality. This further confirms the consolidated hypothesis (Govender and Sivakumar, 2020; Cai et al., 2017; Levy et al., 2010) that the correct assessment of air quality cannot ignore the detailed analysis of the concomitant synoptic and local scale weather conditions.

Finally, the evident improvement of air quality during spring 2020 is attributable to the measures adopted in Italy to limit the pandemic spread of SARS-CoV-2. In Rome, the reduction of private and public mobility due to the closure of commercial activities, industries, and schools, resulted in the correspondent abatement of NO (−43%), NO_2 (−28%), PM_{10} (−18%), and $PM_{2.5}$ (−4%), with respect to the previous years (Campanelli et al., 2021).

3.2. Air pollutant concentrations associated with anemological clustering

This Section analyses the clustering of local atmospheric pollutant concentrations into the three anemological subgroups of wind observations that represent the prevailing weather conditions (Section 2.3). Table 3 reports cluster-averaged concentrations, together with the corresponding deseasonalised intra-cluster STDs. The box plots in Fig. 4 show the distribution of the annual and season-aggregated (autumn-winter from October to March and spring-summer from April to September) cluster-averaged concentrations for the observational sites. Table S2 shows the results of the Mann-Whitney *U* test for the evaluation of inter-cluster differences, at each monitoring station and for each pollutant.

Table 3 shows that SBC is the most populated cluster, followed by SEC and NEC, in this order. The best air quality conditions are observed when the sea breeze develops (SBC), while air pollution worsens in the case of south-easterly flows (SEC), with increases in NO (+78.8%), NO_2 (+250.8%), $PM_{2.5}$ (+11.1%), and PM_{10} (+6.5%), and decreases in the NO_2/NO_x ratio (−2.5%) and O_3 (−15.3%). Air quality further deteriorates for north-easterly flows (NEC), which register an average increase of +201.9% in NO, +286.2% in NO_2, +33.3% in $PM_{2.5}$, and +11.0% in PM_{10}, whereas decrements are observed for the NO_2/NO_x ratio (−8.8%), and O_3 (−30.2%). Variations are always computed with respect to SBC.

Regardless of the cluster and the season, the highest NO (Fig. 4a, g, and 4m) and NO_2 values (Fig. 4b, h, and 4n) are observed in the urban environment, because of the proximity of local sources as vehicular traffic, with generally higher concentrations at CIN than at ADA. In the centre of Rome, inter-cluster variability is always statistically significant (see Table S2). The two rural stations record much lower NO concentrations with statistically significant inter-cluster variation, except for the NEC-SEC case at CDG. The seasonal analysis (Fig. 4a, g, and 4m) shows significant differences between NO concentrations across both clusters and stations, especially in autumn and winter. On the contrary, during the warm months, urban and rural sites exhibit comparable values. The boxplots illustrate how north-easterlies are always and everywhere associated with higher NO concentrations, larger interquartile variability, and larger data excursion.

For NO_2, differences between clusters are always statistically significant at CIN only, while at ADA they only are for the NEC-SBC and the SBC-SEC one-to-one comparisons. As to the rural stations, at ALL results are only significant for the NEC-SEC and SBC-SEC couples, and at CDG for the NEC-SBC and SBC-SEC pairs. The highest mean concentrations are observed in downtown Rome, mainly originating from vehicular traffic and anthropic sources. As for NO, at every station the lowest concentrations are recorded during the summer months, with limited inter-cluster variations. During autumn and winter, NO_2 values increase across clusters, from SBC, to SEC, and finally to NEC.

The annual values of NO_2/NO_x (Fig. 4c) show that urban pollution is significantly affected by wind conditions, with decreasing ratios moving from SBC to SEC, and to NEC. Otherwise, the rural areas seem to be significantly influenced by the regional atmospheric circulation. Also in this case, during spring and summer (Fig. 4o) urban and rural stations experience similar conditions. On the contrary, during autumn and winter (Fig. 4i) the behaviour attributable to environmental conditions is well discernible and the ratio decreases from SBC, to SEC, and to NEC.

Comparatively lower concentrations of O_3 (Fig. 4d, j, and 4p) are observed in downtown Rome with respect to rural areas. The

Table 3
Average concentrations and deseasonalised STDs (in square brackets) for the three meteorological clusters.

Cluster	Days	Occurrence	NO (μg/m^3)	NO_2 (μg/m^3)	NO_2/NO_x (−)	O_3 (μg/m^3)	$PM_{2.5}$ (μg/m^3)	PM_{10} (μg/m^3)
NEC	755	30.4%	15.7 [22.0]	25.1 [7.7]	0.73 [0.07]	47.8 [7.4]	16.8 [8.0]	22.2 [9.4]
SBC	917	37.0%	5.2 [6.5]	6.5 [6.5]	0.80 [0.05]	68.5 [7.9]	12.6 [4.8]	20.0 [6.8]
SEC	810	32.6%	9.3 [9.3]	22.8 [6.6]	0.78 [0.06]	58.0 [8.2]	14.0 [5.0]	21.3 [8.6]

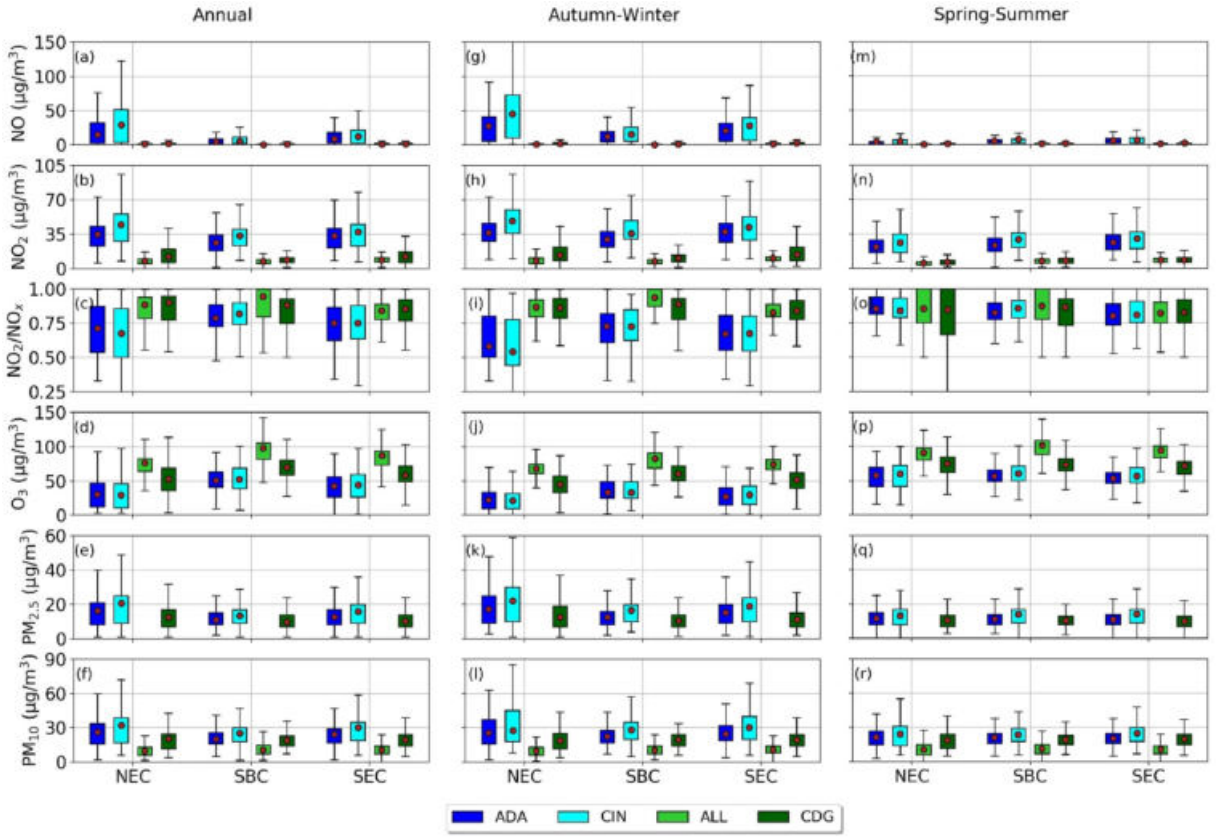

Fig. 4. Average annual (left column) and seasonal (autumn-winter and spring-summer, central and right columns, respectively) box plots of NO (a, g, m), NO_2 (b, h, n), NO_2/NO_x (c, i, o), O_3 (d, j, p), $PM_{2.5}$ (e, k, q), and PM_{10} (f, l, r) for each cluster. The red dots depict the mean values, the lower and upper boundaries of the boxs denote the 25th (Q1) and 75th (Q3) percentiles, and the lower and upper whiskers show the interval between (Q1 – 1.5IQR) and (Q3 + 1.5IQR), where IQR is the interquartile range.

correspondent inter-cluster variations are always statistically significant. The annual boxplots (leftmost panel) illustrate how O_3 concentrations coherently vary across the three different anemological clusters, with values that systematically decrease from the highest (SBC) to the lowest (NEC). The annual average in fact retains the trace of the autumn-winter inter-cluster variability (Fig. 4j), when such behaviour appears to be amplified, while it is less discernible during the warm months (Fig. 4p).

$PM_{2.5}$ (Fig. 4e, k, and 4q) and PM_{10} (Fig. 4f, l, and 4r) concentrations are slightly higher in the city, regardless of the weather systems. For $PM_{2.5}$, the inter-cluster differences are statistically significant for the NEC-SBC pair at all stations, for the NEC-SEC pair at ADA only, and for the SBC-SEC pair at ADA and CIN. For PM_{10}, the statistical significance of the NEC-SBC differences is achieved at all stations except CDG, for the NEC-SEC pair at ALL only, and for the SBC-SEC pair only at the urban sites. In fact, all clusters and all monitoring stations exhibit the highest $PM_{2.5}$ concentrations in autumn-winter. In particular, the increase in concentrations recorded during autumn-winter in correspondence with NEC occurrences is likely attributable to conditions of atmospheric stability and stagnation.

Over the study period 2014–2020, the objective classification of the prevailing local weather regimes into identifiable clusters allows gaining insight into the influence of weather conditions on air quality along the year.

As anticipated in the foregoing analysis of Fig. 4, the climatological behaviour of species concentrations is similar across the three clusters during the warm months (see Fig. 5), while significant differences are detected during autumn and winter. As a matter of fact, clustering allows to selectively amplify the seasonal differences already detected in the monthly time series of the raw data (Fig. 3), and to unambiguously associate them with specific circulation patterns, at the same time better identifying the species that are most affected, notably NO, NO_2, and hence the NO_2/NO_x ratio.

As regards differences across stations, NO values are spatially rather homogeneous from April to September, with negligible or weak (CIN) differences, likely attributable to local transient phenomena (e.g., fires close to the monitoring stations) (ASKANEWS, 2017) as also suggested in the foregoing comment to Fig. 3. Conversely, winter NO concentrations are the lowest for SBC and then increase from SEC to NEC. The presence of NO is virtually undetectable at the rural background stations, suggesting the almost total absence of NO sources outside the urbanised area.

The space-temporal variations of NO_2 are comparable to that of NO: urban stations measure the highest concentrations throughout the year and the impact of anemological conditions is the greatest in winter.

The NO_2 to NO_x ratio significant varies across stations between September and March when the urban environment exhibits the worst air quality conditions. On the other hand, during the warm season NO_2/NO_x values are comparable across stations for SBC and SEC, while northeasterlies appear to allow for larger spatial fluctuations.

O_3 concentrations, consistently with the corresponding time series in Fig. 3, are the highest in rural areas throughout the year. Differences between clusters are more evident in Rome during winter yet the clustering procedure does not appear to significantly amplify different responses of O_3 concentrations to alternative atmospheric conditions.

On the other hand, $PM_{2.5}$ and PM_{10} are both appreciably affected by anemological conditions throughout the year. Trends in concentrations during the year are coherent across stations, confirming the non-local origin of atmospheric particulate.

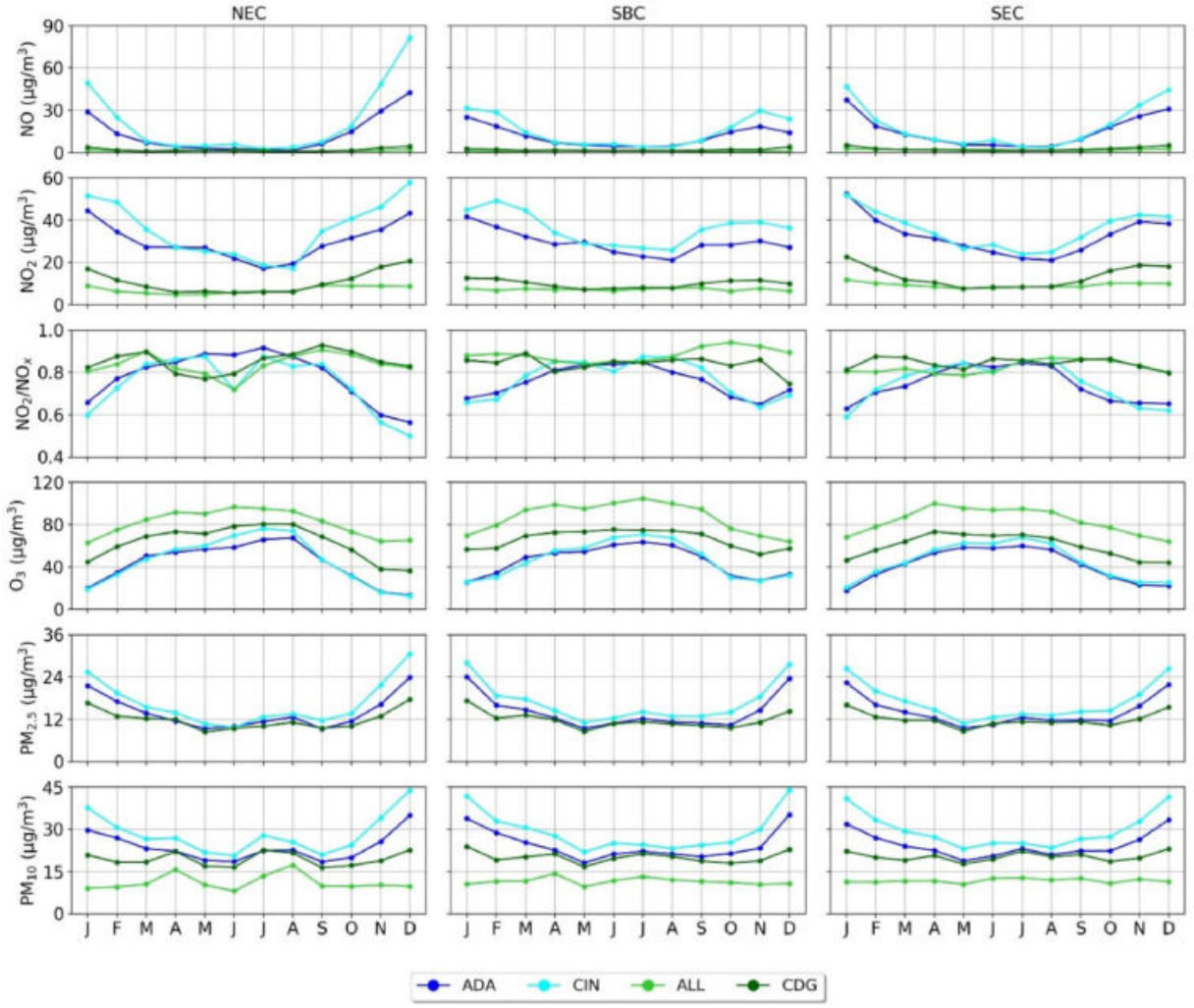

Fig. 5. Monthly-averaged concentrations of NO, NO_2, NO_2/NO_x, O_3, $PM_{2.5}$, and PM_{10} for NEC (left column), SBC (central column), and SEC (right column).

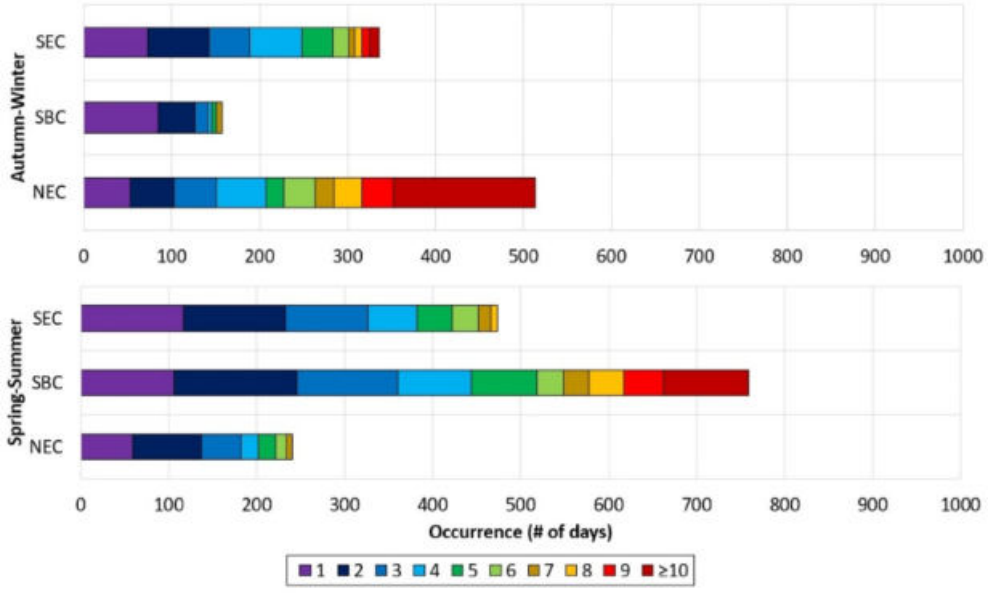

Fig. 6. Distribution of cluster populations (x-axis) with respect to weather persistence (colour scale), in the cold (top panel) and the warm (bottom panel) seasons.

3.3. Relationship between persistence of wind cluster and pollutant concentrations

In this Section, the effect of wind persistence (i.e., the number of consecutive days presenting the same anemological conditions) on atmospheric pollution is analysed, with particular attention to the different responses of urban and rural environments..

For the cold and the warm seasons, Fig. 6 illustrates how the population of each cluster is distributed with respect to persistence, highlighting significant differences across clusters. SEC is more frequently experienced in spring and summer, when the same wind regime is liable to last no more than three/four days, although longer events can occur up to a duration of seven days. The number of cases does not seem to be affected by seasonality. SBC is the most populated cluster in spring and summer when the sea breeze circulation can persist for up to two consecutive weeks. The probability of occurrence of SBC

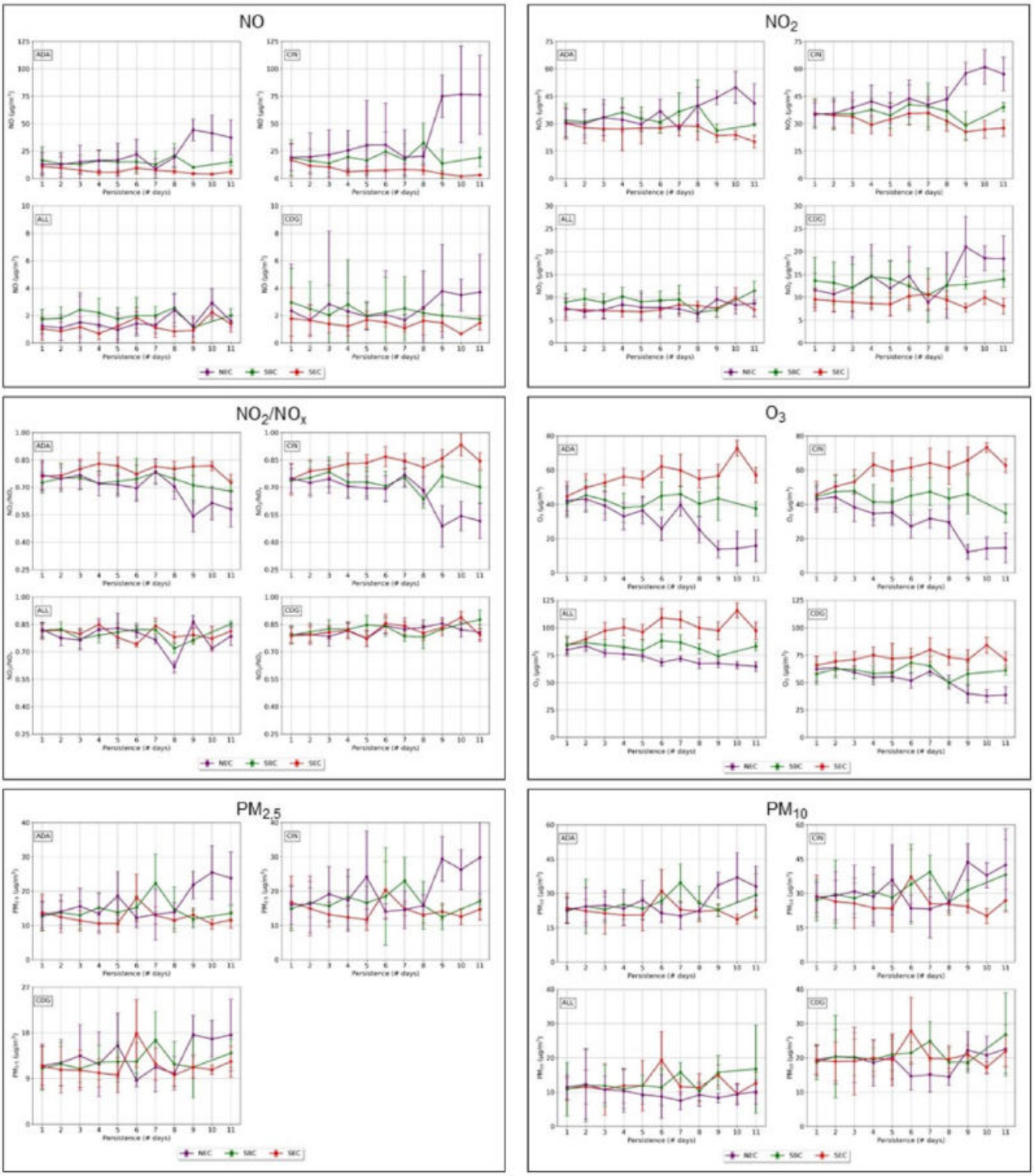

Fig. 7. Pollutant concentrations (μg/m^3, y-axis) as a function of cluster persistence (number of consecutive days, x-axis) for ADA, CIN, ALL, and CDG stations. NO (upper left), NO_2 (upper right), NO_2/NO_x (central left), O_3 (central right), $PM_{2.5}$ (lower left), and PM_{10} (lower right) are shown. The error bars show the associated deseasonalised STDs.

decreases during the cold months, when this regime seldom persists for more than two days. On the contrary, NEC prevails in autumn and winter, with a high incidence of conditions lasting for at least ten days. In both seasons, the two secondary clusters are characterised by event populations that significantly decrease as persistence increases, thus recommending handling the results obtained for the under-sampled events longer than six days with a great deal of caution.

Fig. 7 presents annual pollutant concentrations as a function of cluster persistence. For NO (Fig. 7, upper left panel), the urban stations show lower values for SEC with respect to SBC and NEC. Average concentrations corresponding to one-day events appear to be independent of the meteorological cluster, while those corresponding to longer durations can significantly differ. In downtown Rome, NO concentrations can either decrease as persistence increases (SEC), fluctuate around an almost constant level (SBC), or markedly increase (NEC), although in association with higher STDs. At the rural stations, the concentrations are very low (always below 4 $\mu g/m^3$) and are characterised by considerable uncertainty, especially at CDG. Although north-easterlies (NEC events) that persist for $7 \div 10$ days are associated with higher STDs, they have been verified to constitute a statistically significant sample, with mean concentrations that are in line with those found for shorter durations.

NO_2 values (Fig. 7, upper right panel) are, on average, higher at CIN than at ADA, yet average concentrations are very similar for one-day events and tend to diverge for longer persistence slowly. In downtown Rome, NO_2 values are the lowest for SEC, while SBC and NEC are characterised by similar concentrations. At ALL, concentrations associated with NEC and SEC events shorter than seven days almost coincide, while they are slightly higher for SBC. Conversely, at CDG, the lowest average concentrations correspond to SEC events, while NEC and SBC generate similar pollution conditions for events that last up to eight days.

The NO_2 to NO_x ratio (Fig. 7, central left panel) shows significant differences as both the wind conditions and their persistence vary, especially in the city. SEC events are associated with the highest values, while the lower scores of SBC and NEC events show comparable trends up to eight-day durations, to then diverge. On the other hand, rural stations seem not to be affected by alternative meteorological conditions, nor by their persistence.

The effect of the weather regime persistence is particularly evident for O_3 (Fig. 7, central right panel). For one-day events, O_3 values seem to be virtually independent of the atmospheric dynamics, yet, as duration increases, the three different weather regimes give rise to divergent trends. This behaviour is very marked in the urban environment. The rural sites show similar curves, although with higher O_3 levels and more limited inter-cluster differences.

$PM_{2.5}$ (Fig. 7, lower left panel) and PM_{10} (Fig. 7, lower right panel) show the same behaviour, regardless of anemological conditions and persistence. Only the NEC events, when lasting over nine days, determine a net increase in the particulate content.

4. Discussion

The results suggest that synoptic and local circulation systems play a major role in governing in-situ air quality conditions. In fact, although atmospheric chemistry processes and weather variables (such as specific humidity and air temperature) are not here considered, surface anemological data are probably the most widely available meteorological parameters. Data can be provided by capillary networks even in urban areas and data are often accessible from the web through national and international networks. It follows that the wind input data for the clustering can be easily found and, therefore, it is possible to estimate the pollution level with high spatial-temporal resolution.

This approach has already proven successful in several studies. E.g., Darby (2005) used hourly surface wind data acquired in Houston (USA) to identify wind patterns coincident with the maximum daily ozone concentration. Hsu and Cheng (2016) classified the weather patterns in Taiwan from average daily surface wind data, underlining their influence on the concentration of particulate matters. Li et al. (2020) studied the relationship between the onset of the breeze and the ozone level in Houston (USA) through k-means anemological clustering. Finally, Xie et al. (2022) evaluated the impact of the steadiness and duration of urban surface wind patterns on air quality in terms of NO_2 and particulate matters in Shenzhen (China), highlighting the importance of determining wind clusters to improve the air quality forecasting and strategic decisions on air pollution emergencies.

As summarised in Table 3, the most unfavourable meteorological pattern occurs when the synoptic conditions give rise to prevailing winds from the northeast for the entire duration of the day, preventing the development of the sea breeze. In this case, the northern synoptic winds worsen the air quality at the ground level, as they can advect pollutants from external sources along the Tiber valley towards the urban area of Rome. This condition frequently occurs during the cold months, when synoptic and local anemological conditions govern air pollutant dispersion. As highlighted in Fig. 6, during winter, atmospheric stability can persist for several consecutive days, because of the development of thermal inversion layers that limit the development of the mixed layer (Gobbi et al., 2007). In this case, locally emitted substances are confined within a small volume of the atmosphere, resulting in the highest surface-level concentrations. In Rome, this situation mainly affects the NO and NO_2 levels. On the contrary, the development of the sea breeze ensures the best air quality conditions, giving rise to the inland advection of clean air masses, and to air recirculation as a consequence of the change in wind direction during the onset of the sea breeze front. The sea breeze is identifiable in the region throughout the year (Petenko et al., 2011; Di Bernardino et al., 2021b), although it is prevalent during the warm months when this regime can dominate the atmospheric dynamics for several consecutive days. On the other hand, in the case of prevailing winds from the southeast, poor air quality levels are recorded, especially in terms of particulate matters, as southerly winds can advect high quantities of suspended particulate from the Saharan desert. The SEC events have limited duration and are therefore responsible for limited increases in the concentrations of atmospheric pollutants. In general, enhanced persistence induces the largest inter-cluster differences, although uncertainties can be large and under-sampling can represent an issue.

As reported in Table 3, NO and NO_2 concentrations are reduced by approximately 66.9% and 74.1% for SBC with respect to NEC, while significant but smaller reductions are recorded for $PM_{2.5}$ (−25.0%), and PM_{10} (−9.9%). O_3 levels and the NO_2 to NO_x ratio on average respectively increase by +43.3% and +9.6% from NEC to SBC. Rural stations record NO and NO_2 concentrations that are much lower than in the urban area, due to their distance from point sources. This implies that their values are often close to the instrumental measurement thresholds (0.50 $\mu g/m^3$ and 0.75 $\mu g/m^3$ for NO and NO_2, respectively) and, consequently, that their variability is restrained.

Variations in NO_2 and NO concentrations clearly influence NO_2/NO_x. The highest NO_2/NO_x values observed at rural sites suggest low NO levels in the non-urban environment and increased secondary formation of NO_2 through photochemical atmospheric reactions. On the contrary, the high NO_2/NO_x values experienced in the urban environment suggest that the main source of NO_x is the NO_2 emitted by vehicular traffic, regardless of the meteorological conditions. The assessment of NO_2/NO_x and the discussion about the main NO_2 sources are particularly interesting, as they may affect the efficiency of NO_x control measures, which need to be established and appropriately applied based on the percentage of NO_2 with respect to the total atmospheric NO_x (Carslaw and Beevers, 2004). For instance, several researchers (e.g., Carslaw, 2005; Grice et al., 2009) have analysed the impact of primary NO_2 emissions from vehicular traffic in many European cities. Their results show an upward NO_2/NO_x trend attributable to the wide use of diesel vehicles and the increased use of diesel particulate filters and oxidation catalysts.

Moreover, the NO_2 to NO_x ratios found in this study (0.50–0.95) are well above the range of the emission ratios (0.03–0.22) proposed for the exhaust (Preble et al., 2015), reasonably due to the shorter atmospheric lifetime of NO compared to NO_2, but in agreement with the 0.24–0.75 range found by Zeng et al. (2022).

The assessment of the link between ozone concentrations and circulation patterns is undoubtedly more complicated: emitted precursors, i.e., NO_x and volatile organic compounds (VOCs), which are connected by complex nonlinear photochemistry (Liu and Shi, 2021), directly drive the formation of O_3. The combined action of higher NO_x concentrations and VOCs in the atmosphere and the presence of solar radiation gives rise to the photolysis reactions of nitrogen dioxide into nitrogen monoxide and an oxygen radical. The latter, reacting with the oxygen molecules present in the atmosphere, produces ozone, thus increasing the levels measured at the ground. Furthermore, the removal of O_3 is favoured during night-time and near very large emissions of NO through the process of NO_x titration, consisting in the removal of O_3 through reaction with NO (Liu and Shi, 2021). Unfortunately, continuous VOCs measurements are not available in the region of interest, and this analysis is therefore forced to neglect their effect. In the investigated area, the highest ozone concentrations are experienced in concomitance of prevailing north-easterlies (NEC), while the lowest O_3 concentrations are observed for south-easterly winds (SEC), due to their ability to carry clean marine air masses inland, favouring pollutants dispersion. Finally, when the local circulation is dominant, intermediate but rather high concentrations of O_3 are measured, as induced by both the stagnation conditions and the pollution recirculation by wind rotation (Ngan and Byun, 2011) that characterise the sea breeze regime (SBC) (Di Bernardino et al., 2022a). Our results agree with the findings by Li et al. (2020), who linked alternative wind clusters with variations in surface and aircraft ozone measurements in Houston (U.S.A.), obtaining maximum/minimum ozone values in low/high ventilation conditions.

Finally, the limited spatial variability of particulate matter concentrations is attributable to the superposition of multiple effects. As reported by Dimitriou and Kassomenos (2014), high PM concentrations can be detected in Rome both in the case of north-easterly winds, coming from Central Europe and the Balkanic Peninsula, and crossing the Adriatic Sea, and in the case of southerly winds, which can advect high concentrations of desert dust (Gobbi et al., 2019). Even in the case of sea breeze onset, homogeneous PM concentration can be justified by considering the advection of marine spray. Marine aerosols generally contain coarser particles compared to those of anthropogenic origin and can therefore contribute to the increase in PM_{10} concentration (Gerasopoulos et al., 2011). Nonetheless, the highest concentrations of both PM_{10} and $PM_{2.5}$ are measured in Rome downtown, where emissions from local anthropogenic sources add up to the medium-long range contribution. Furthermore, it must be considered that the proposed anemological clustering is only based on wind intensity and direction, without considering, e.g., rainy days and the consequent washout effect on atmospheric pollutants and particulate matters.

Unfortunately, since only daily averaged concentrations are available from the database, it is not possible to assess the impact of anemological conditions on the probability of exceeding the threshold concentrations imposed by European Directives (EU, 1999; EU, 2008), with limits that can be either annual (NO_2, $PM_{2.5}$, and PM_{10}), daily (PM_{10}), 8-h mean (O_3), or hourly (NO_2) (EU, 1999; EU, 2008).

5. Conclusions

In this study, the relationship between synoptic and local scale anemological conditions and the in-situ concentrations of the main atmospheric pollutants (NO, NO_2, NO_2/NO_x, O_3, $PM_{2.5}$, and PM_{10}), in downtown Rome and its rural surroundings, is investigated for the 2014–2020 period. A k-means clustering technique allowed the identification of the prevailing local circulation patterns, by only using surface wind velocity and direction collected by coastal weather stations, following a procedure widely used in the literature. Three typical clusters were recognised: the Northeasterly cluster (NEC), dominated by the synoptic circulation and characterised by prevailing winds from the Northeast for the entire duration of the day; the Sea Breeze Cluster (SBC), when weather conditions at the local scale permit the onset of the sea breeze regime during the daytime, and the Southeasterly Cluster (SEC), arising from the superposition of the synoptic and local circulation and by the weakening of the sea breeze onset, as induced by south-easterly synoptic winds.

Our findings show a significant impact of the alternative weather regimes on in-situ air quality, both in downtown Rome and in the surrounding region. In particular, NEC corresponds to the highest levels of atmospheric pollution over the whole area, while during the SBC events, the development of the sea breeze ensures pollutants dispersion through clean sea air advection. The largest differences between NEC and SBC are recorded for NO_2 concentrations, which increase by +286.2%, followed by NO (+201.9%), $PM_{2.5}$ (+33.3%), and PM_{10} (+11.0%). Conversely, O_3 levels and the NO_2/NO_x ratio exhibit a decrease of −30.2%, and −8.8%, respectively. In the case of SEC, quite poor air quality conditions are observed: atmospheric pollution is reduced by the contribution of marine, clean air masses but can be worsened by the compensating effect of Saharan desert dust advection, which can cause sudden temporary increases in the concentration of particulate matters.

The differences between the alternative regimes represented by clusters are particularly evident during winter, when NEC events can persist for more than ten days. During NEC events, NO and NO_2 reach the highest concentrations, with a maximum increase of +240.6% with respect to SBC in December, while differences as large as +56.5% are commonly detected (e.g., at the CIN urban station). The local air quality degrades for NEC events all over the region, also leading to the lowest O_3 levels, which are reduced by 60.2% at CIN in December with respect to SBC. $PM_{2.5}$ and PM_{10} appear to be differently affected by the alternative regimes: inter-cluster differences vanish, although a strong dependence on seasonality is still observable. Peaks are observed during cold month, when the persistent atmospheric stability limits the development of the mixed layer, giving rise to an increase in pollution at the ground level.

The results of the present work strongly support studies delving into atmospheric pollution be combined with the thorough characterisation of local anemological conditions, to appropriately support the design and implementation of effective atmospheric pollutant abatement strategies. Furthermore, the proposed method makes it possible to estimate the pollution levels expected in conjunction with peculiar wind conditions. The adoption of this approach, both in the absence or in combination with more sophisticated tools (e.g., dispersion models), can provide policymakers with useful indications as to the most effective pollution mitigation actions. Moreover, the coupled installation of weather and air quality sensors, sharing the same instrumental characteristics and homogeneously distributed in the urban and rural environment of interest, would further permit to typify local emissions, estimate their long-range advection, and investigate the correlation between air quality and weather conditions. A synergistic and accurate assessment of emission sources, atmospheric dynamics, and chemistry is essential to correctly evaluate the effectiveness of pollution mitigation policies. As highlighted in this work, atmospheric dynamics differently affect atmospheric pollution, depending on the selected species, the investigated season, and the persistence of weather conditions. Future research should combine in-situ measurements with satellite products (e.g., columnar content retrieval), and vertical profiles of air contaminants, allowing for a comprehensive and in-depth analysis of the processes occurring not only at the ground layer but in the entire vertical extent of the planetary boundary layer.

Credit author statement

Annalisa Di Bernardino: Conceptualization, Software, Validation, Formal analysis, Investigation, Data Curation, Writing - Original Draft,

Visualization. Anna Maria Iannarelli: Methodology, Data Curation, Writing - Review & Editing, Project administration. Stefano Casadio: Methodology, Validation, Formal analysis, Resources, Writing - Review & Editing, Project administration, Funding acquisition. Giovanna Pisacane: Conceptualization, Writing - Review & Editing. Anna Maria Siani: Conceptualization, Writing - Review & Editing, Supervision.

Declaration of competing interest

The authors declare that they have no known competing financial interests or personal relationships that could have appeared to influence the work reported in this paper.

Acknowledgements

The authors gratefully acknowledge ARPA Lazio for providing air quality data used in this publication. This research was supported by BAQUNIN Project team, funded by ESA through the contract ID 4000126749/19/I-NS.

Appendix A. Supplementary data

Supplementary data to this article can be found online at https://doi.org/10.1016/j.apr.2023.101670.

References

Allwine, K.J., Whiteman, C.D., 1994. Single-station integral measures of atmospheric stagnation, recirculation and ventilation. Atmos. Environ. 28 (4), 713–721. https://doi.org/10.1016/1352-2310(94)90048-5.

ASKANEWS, 2017. https://www.askanews.it/cronaca/2017/08/03/incendi-da-questa-mattina-130-interventi-vigili-fuoco-roma-pn_20170803_00295/. (Accessed 15 September 2022) (last accessed on.

Beck, H.E., Zimmermann, N.E., McVicar, T.R., Vergopolan, N., Berg, A., Wood, E.F., 2018. Present and future Köppen-Geiger climate classification maps at 1-km resolution. Sci. Data 5 (1), 1–12. https://doi.org/10.1038/sdata.2018.214.

Bower, J.S., Broughton, G.F.J., Willis, P.G., 1993. Measurements of urban photochemical oxidants. Spec. Publ. Roy. Soc. Chem. 115, 23.

Cai, W, Li, K, Liao, H, Wang, H, Wu, L, 2017. Weather conditions conducive to Beijing severe haze more frequent under climate change. Nat Climate Change 7, 257.

Calmanti, S., Dell'Aquila, A., Maimone, F., Pelino, V., 2015. Evaluation of climate patterns in a regional climate model over Italy using long-term records from SYNOP weather stations and cluster analysis. Clim. Res. 62 (3), 173–188. https://doi.org/10.3354/cr01256.

Campanelli, M., Iannarelli, A.M., Mevi, G., Casadio, S., Diémoz, H., Finardi, S., Dinoi, A., Castelli, E., Di Sarra, A., Di Bernardino, A., Casasanta, G., Bassani, C., Siani, A.M., Cacciani, M., Barnaba, F., Di Liberto, L., Argentini, S., 2021. A wide-ranging investigation of the COVID-19 lockdown effects on the atmospheric composition in various Italian urban sites (AER–LOCUS). Urban Clim. 39, 100954 https://doi.org/10.1016/j.uclim.2021.100954.

Carslaw, D.C., 2005. Evidence of an increasing NO2/NOx emissions ratio from road traffic emissions. Atmos. Environ. 39 (26), 4793–4802. https://doi.org/10.1016/j.uclim.2021.100954.

Carslaw, D.C., Beevers, S.D., 2004. New Directions: should road vehicle emissions legislation consider primary NO2? Atmos. Environ. 38 (8), 1233–1234. https://doi.org/10.1016/j.atmosenv.2003.12.008.

Carslaw, D.C., Beevers, S.D., Tate, J.E., Westmoreland, E.J., Williams, M.L., 2011. Recent evidence concerning higher NOx emissions from passenger cars and light duty vehicles. Atmos. Environ. 45, 7053–7063. https://doi.org/10.1016/j.atmosenv.2011.09.063.

Darby, L.S., 2005. Cluster analysis of surface winds in Houston, Texas, and the impact of wind patterns on ozone. J. Appl. Meteorol. Climatol. 44 (12), 1788–1806. https://doi.org/10.1175/JAM2320.1.

Di Bernardino, A., Iannarelli, A.M., Casadio, S., Perrino, C., Barnaba, F., Tofful, L., Campanelli, M., Di Liberto, L., Mevi, G., Siani, A.M., Cacciani, M., 2021a. Impact of synoptic meteorological conditions on air quality in three different case studies in Rome, Italy. Atmos. Pollut. Res. 12 (4), 76–88. https://doi.org/10.1016/j.apr.2021.02.019.

Di Bernardino, A., Iannarelli, A.M., Casadio, S., Mevi, G., Campanelli, M., Casasanta, G., Cede, A., Tiefengraber, M., Siani, A.M., Spinei, E., Cacciani, M., 2021b. On the effect of sea breeze regime on aerosols and gases properties in the urban area of Rome. Italy. Urban Clim. 37, 100842 https://doi.org/10.1016/j.uclim.2021.100842.

Di Bernardino, A., Iannarelli, A.M., Casadio, S., Pisacane, G., Mevi, G., Cacciani, M., 2022a. Classification of synoptic and local-scale wind patterns using k-means clustering in a Tyrrhenian coastal area (Italy). Meteorol. Atmos. Phys. 134 (2), 1–12. https://doi.org/10.1007/s00703-022-00871-z.

Di Bernardino, A., Iannarelli, A.M., Diémoz, H., Casadio, S., Cacciani, M., Siani, A.M., 2022b. Analysis of two-decade meteorological and air quality trends in Rome (Italy). Theor. Appl. Climatol. 149, 291–307. https://doi.org/10.1007/s00704-022-04047-y.

Dimitriou, K., Kassomenos, P., 2014. Indicators reflecting local and transboundary sources of PM2.5 and PMCOARSE in Rome–Impacts in air quality. Atmos. Environ. 96, 154–162. https://doi.org/10.1016/j.atmosenv.2014.07.029.

EU, 1999. Council Directive 1999/30/EC of 22 April 1999 relating to limit values for sulphur dioxide, nitrogen dioxide and oxides of nitrogen, particulate matter and lead in ambient air.

EU, 2008. Directive 2008/50/EC of the European Parliament and of the Council of 21 May 2008 on ambient air quality and cleaner air for Europe.

European Environmental Agency, 2021. Air Quality in Europe 2021, Report No. 15/2021. https://doi.org/10.2800/549289.

Fountoulakis, I., Diémoz, H., Siani, A.M., Laschewski, G., Filippa, G., Arola, A., Bais, A.F., De Backer, H., Lakkala, K., Webb, A.R., De Bock, V., Karppinen, T., Garane, K., Kapsomenakis, J., Koukouli, M.-E., Zerefos, C.S., 2019. Solar UV irradiance in a changing climate: trends in Europe and the significance of spectral monitoring in Italy. Environments 7 (1), 1. https://doi.org/10.3390/environments7010001.

Gerasopoulos, E., Amiridis, V., Kazadzis, S., Kokkalis, P., Eleftheratos, K., Andreae, M.O., Andreae, T.W., El-Askary, H., Zerefos, C.S., 2011. Three-year ground based measurements of aerosol optical depth over the Eastern Mediterranean: the urban environment of Athens. Atmos. Chem. Phys. 11 (5), 2145–2159. https://doi.org/10.5194/acp-11-2145-2011.

Gobbi, G.P., Barnaba, F., Ammannato, L., 2007. Estimating the impact of Saharan dust on the year 2001 PM10 record of Rome. Italy. Atmos. Environ. 41 (2), 261–275. https://doi.org/10.1016/j.atmosenv.2006.08.036.

Gobbi, G.P., Angelini, F., Barnaba, F., Costabile, F., Baldasano, J.M., Basart, S., Sozzi, R., Bolignano, A., 2013. Changes in particulate matter physical properties during Saharan advections over Rome (Italy): a four-year study, 2001–2004. Atmos. Chem. Phys. 13 (15), 7395–7404. https://doi.org/10.5194/acp-13-7395-2013.

Gobbi, G.P., Barnaba, F., Di Liberto, L., Bolignano, A., Lucarelli, F., Nava, S., Perrino, C., Pietrodangelo, A., Basart, S., Costabile, F., Dionisi, D., Rizza, U., Canepari, S., Sozzi, R., Morelli, M., Manigrasso, M., Drewnick, F., Struckmeier, C., Poenitz, K., Wille, H., 2019. An inclusive view of Saharan dust advections to Italy and the Central Mediterranean. Atmos. Environ. 201, 242–256. https://doi.org/10.1016/j.atmosenv.2019.01.002.

Govender, P., Sivakumar, V., 2020. Application of k-means and hierarchical clustering techniques for analysis of air pollution: a review (1980–2019). Atmos. Pollut. Res. 11 (1), 40–56. https://doi.org/10.1016/j.apr.2019.09.009.

Grice, S., Stedman, J., Kent, A., Hobson, M., Norris, J., Abbott, J., Cooke, S., 2009. Recent trends and projections of primary NO2 emissions in Europe. Atmos. Environ. 43 (13), 2154–2167. https://doi.org/10.1016/j.atmosenv.2009.01.019.

Hartigan, J.A., Wong, M.A., 1979. Algorithm AS 136: a k-means clustering algorithm. J. R. Stat. Soc. Ser. C Appl. Stat. 28 (1), 100–108.

Hess, P., Brezowsky, H., 1977. Katalog der Grosswetterlagen Europas 1881–1976, 3. verbesserte und ergänzte Aufl. Berichte des Deutschen Wetterdienstes 113, 1–140.

Hsu, C.H., Cheng, F.Y., 2016. Classification of weather patterns to study the influence of meteorological characteristics on PM2.5 concentrations in Yunlin County, Taiwan. Atmos. Environ. 144, 397–408. https://doi.org/10.1016/j.atmosenv.2016.09.001.

Hsu, C.H., Cheng, F.Y., 2019. Synoptic weather patterns and associated air pollution in Taiwan. Aerosol Air Qual. Res. 19 (5), 1139–1151. https://doi.org/10.4209/aaqr.2018.09.0348.

ISPRA, 2014. Linee guida per le attività di assicurazione/controllo qualità (QA/QC) per le reti di monitoraggio per la qualità dell'aria ambiente, ai sensi del D.Lgs. 155/2010 come modificato dal D.Lgs. 250/2012.

ISTAT, 2020. https://www.istat.it/en/censuses/population-and-housing/results. (Accessed 15 July 2022) (last accessed on.

ISTAT, 2021. Italian Statistical Yearbook: Tourism. https://www.istat.it/storage/ASI/2021/capitoli/C19.pdf. (Accessed 20 July 2022) (last accessed on.

Jain, A.K., Murty, M.N., Flynn, P.J., 1999. Data clustering: a review. ACM Comput. Surv. 31 (3), 264–323. https://doi.org/10.1145/331499.331504.

Jia, J., Cheng, S., Liu, L., Lang, J., Wang, G., Chen, G., Liu, X., 2017. An integrated WRF-CAMx modeling approach for impact analysis of implementing the emergency PM2.5 control measures during red alerts in Beijing in December 2015. Aerosol Air Qual. Res. 17 (10), 2491–2508. https://doi.org/10.4209/aaqr.2017.01.0009.

Kijewska, A., Bluszcz, A., 2016. Research of varying levels of greenhouse gas emissions in European countries using the k-means method. Atmos. Pollut. Res. 7 (5), 935–944. https://doi.org/10.1016/j.apr.2016.05.010.

Kodinariya, T.M., Makwana, P.R., 2013. Review on determining number of cluster in K-means clustering. Int. J. 1 (6), 90–95.

Kukkonen, J., Pohjola, M., Sokhi, R.S., Luhana, L., Kitwiroon, N., Fragkou, L., Rantamäki, M., Berge, E., Ødegaard, V., Slørdal, L.H., Denby, B., Finardi, S., 2005. Analysis and evaluation of selected local-scale PM10 air pollution episodes in four European cities: helsinki, London, Milan and Oslo. Atmos. Environ. Times 39 (15), 2759–2773. https://doi.org/10.1016/j.atmosenv.2004.09.090.

Lamb, H.H., 1972. British Isles weather types and a register of the daily sequence of circulation patterns 1861-1971. Geophysical Memoirs.

Lazio, A.R.P.A., 2014. Daily Bulletin, Reference Day: 01.12.2014. http://www.arpalazio.net/main/aria/sci/basedati/bquotidiano/2014/20141201CRQA.pdf. (Accessed 20 July 2022) (last accessed on.

Lazio, A.R.P.A., 2016. http://www.arpalazio.net/main/aria/sci/basedati/chimici/chimici.php. (Accessed 20 July 2022) last accessed on.

Lelieveld, J., Evans, J.S., Fnais, M., Giannadaki, D., Pozzer, A., 2015. The contribution of outdoor air pollution sources to premature mortality on a global scale. Nature 525 (7569), 367–371. https://doi.org/10.1038/nature15371.

Levy, I., Dayan, U., Mahrer, Y., 2010. Differing atmospheric scales of motion and their impact on air pollutants. Int. J. Climatol. 30 (4), 612–619. https://doi.org/10.1002/joc.1905.

Li, W., Wang, Y., Bernier, C., Estes, M., 2020. Identification of sea breeze recirculation and its effects on ozone in Houston, TX, during DISCOVER-AQ 2013. J. Geophys. Res. Atmos. 125 (22), e2020JD033165 https://doi.org/10.1029/2020JD033165.

Liu, C., Shi, K., 2021. A review on methodology in O3-NOx-VOC sensitivity study. Environ. Pollut. 291, 118249 https://doi.org/10.1016/j.envpol.2021.118249.

Lovett, G.M., Tear, T.H., Evers, D.C., Findlay, S.E., Cosby, B.J., Dunscomb, J.K., Driscoll, C.T., Weathers, K.C., 2009. Effects of air pollution on ecosystems and biological diversity in the eastern United States. Ann. N. Y. Acad. Sci. 1162 (1), 99–135. https://doi.org/10.1111/j.1749-6632.2009.04153.x.

Mann, H.B., Whitney, D.R., 1947. On a test of whether one of two random variables is stochastically larger than the other. Ann. Math. Stat. 50–60.

Ministry for Environment, Land and Sea Protection of Italy, 2017. Quality Assurance Procedures to Verify Compliance with the Quality of Ambient Air Measurements, Carried Out in the Stations of the Measurement Networks. https://www.gazzettaufficiale.it/eli/id/2017/04/26/17A02825/sg. (Accessed 20 July 2022) (last accessed on.

Mujtaba, G., Shahzad, S.J.H., 2021. Air pollutants, economic growth and public health: implications for sustainable development in OECD countries. Environ. Sci. Pollut. Res. 28 (10), 12686–12698. https://doi.org/10.1007/s11356-020-11212-1.

Ngan, F., Byun, D., 2011. Classification of weather patterns and associated trajectories of high-ozone episodes in the Houston–Galveston–Brazoria area during the 2005/06 TexAQS-II. J. Appl. Meteorol. Climatol. 50 (3), 485–499. https://doi.org/10.1175/2010JAMC2483.1.

Palmieri, S., Durante, G., Siani, A.M., Casale, G.R., 2008. Atmospheric stagnation episodes and hospital admissions. Publ. Health 122 (10), 1128–1130. https://doi.org/10.1016/j.puhe.2008.02.006.

Petenko, I., Mastrantonio, G., Viola, A., Argentini, S., Coniglio, L., Monti, P., Leuzzi, G., 2011. Local circulation diurnal patterns and their relationship with large-scale flows in a coastal area of the Tyrrhenian Sea. Bound.-Lay. Meteorol. 139 (2), 353–366. https://doi.org/10.1007/s10546-010-9577-x.

Preble, C.V., Dallmann, T.R., Kreisberg, N.M., Hering, S.V., Harley, R.A., Kirchstetter, T. W., 2015. Effects of particle filters and selective catalytic reduction on heavy-duty diesel drayage truck emissions at the Port of Oakland. Environ. Sci. Technol. 49 (14), 8864–8871. https://doi.org/10.1021/acs.est.5b01117.

Ravina, M., Caramitti, G., Panepinto, D., Zanetti, M., 2022. Air quality and photochemical reactions: analysis of NOx and NO2 concentrations in the urban area of Turin, Italy. Air Qual. Atmos. Health 15 (3), 541–558. https://doi.org/10.1007/s11869-022-01168-1.

Reuters, 2015. https://www.reuters.com/article/us-italy-environment-fireworks-idUSKBN0UD1IN20151230. (Accessed 20 July 2022) last accessed on.

Riccio, A., Giunta, G., Chianese, E., 2007. The application of a trajectory classification procedure to interpret air pollution measurements in the urban area of Naples (Southern Italy). Sci. Total Environ. 376 (1–3), 198–214. https://doi.org/10.1016/j.scitotenv.2007.01.068.

Richmond-Bryant, J., Chris Owen, R., Graham, S., Snyder, M., McDow, S., Oakes, M., Kimbrough, S., 2017. Estimation of on-road NO2 concentrations, NO2/NOX ratios, and related roadway gradients from near-road monitoring data. Air Qual. Atmos. Health 10 (5), 611–625. https://doi.org/10.1007/s11869-016-0455-7.

Scott, A.J., 2021. The longevity economy. The Lancet Healthy Longevity 2 (12), e828–e835. https://doi.org/10.1016/S2666-7568(21)00250-6.

Squizzato, S., Masiol, M., 2015. Application of meteorology-based methods to determine local and external contributions to particulate matter pollution: a case study in Venice (Italy). Atmos. Environ. 119, 69–81. https://doi.org/10.1016/j.atmosenv.2015.08.026.

Tian, D., Fan, J., Jin, H., Mao, H., Geng, D., Hou, S., Zang, P., Zhang, Y., 2020. Characteristic and spatiotemporal variation of air pollution in Northern China based on correlation analysis and clustering analysis of five air pollutants. J. Geophys. Res. Atmos. 125 (8), e2019JD031931 https://doi.org/10.1029/2019JD031931.

Wilcoxon, F., 1949. Some Rapid Approximate Statistical Procedures Stamford. Conn American Cyanamid Co.

Williams, M.L., Carslaw, D.C., 2011. New directions: science and policy – out of step on NOx and NO2? Atmos. Environ. 45, 3911–3912. https://doi.org/10.1016/j.atmosenv.2011.04.067.

Xiang, S., Zhang, S., Wang, H., Yu, Y.T., Wallington, T.J., Shen, W., Kirchner, U., Deng, Y., Tan, Q., Zhou, Z., Wu, Y., 2022. Variability of NO2/NOx ratios in multiple microenvironments from on-road and near-roadway measurements. ACS EST Engg 2, 1599–1610. https://doi.org/10.1021/acsestengg.2c00027.

Xie, J., Sun, T., Liu, C., Li, L., Xu, X., Miao, S., Lin, L., Chen, Y., Fan, S., 2022. Quantitative evaluation of impacts of the steadiness and duration of urban surface wind patterns on air quality. Sci. Total Environ. 850, 157957 https://doi.org/10.1016/j.scitotenv.2022.157957.

Yu, C., Zhao, T., Bai, Y., Zhang, L., Kong, S., Yu, X., He, J., Cui, C., Yang, J., You, Y., Ma, G., Wu, M., Chang, J., 2020. Heavy air pollution with a unique “non-stagnant” atmospheric boundary layer in the Yangtze River middle basin aggravated by regional transport of PM 2.5 over China. Atmos. Chem. Phys. 20 (12), 7217–7230. https://doi.org/10.5194/acp-20-7217-2020.

Zeng, L., Yang, J., Guo, H., Lyu, X., 2022. Impact of NOx reduction on long-term surface ozone pollution in roadside and suburban Hong Kong: field measurements and model simulations. Chemosphere 302, 134816. https://doi.org/10.1016/j.chemosphere.2022.134816.